A Novel Wideband Compact Microstrip Coupled-Line Ring Hybrid for Arbitrarily High Power-Division Ratios

Hee-Ran Ahn, *Senior Member, IEEE*, and Manos M. Tentzeris, *Fellow, IEEE*

***Abstract*—This brief introduces a novel, compact, and wideband coupled-line ring hybrid configuration that allows for the easy realization of arbitrarily high power-division ratios featuring significant miniaturization and wider bandwidths compared with other commonly utilized implementations. The circumference of a proof-of-concept 12-dB power-division ratio prototype is 209.3° long, which occupies 15% of the conventional area, and the measured bandwidth of the 15-dB return loss is 78%, which is an improvement by a factor around 1.8.**

***Index Terms*—Arbitrary power-division ratios, compact ring hybrids, coupled-line ring hybrids, high power-division ratios, rat-race couplers, symmetric equivalent circuits, wideband ring hybrids.**

I. Introduction

THE ring hybrids [1]–[9], which are also commonly called "rat-race couplers," have been extensively used for various applications, such as balanced amplifiers [10] and antenna arrays, typically necessitating the easy realization of arbitrary power-division ratios [11]. In addition, as numerous multifunctional wireless modules require a substantial reduction in mass and volume, the compactness of the ring hybrids has been of high interest. Typical ring hybrid topologies consist of three 90° and one 270° transmission-line sections (TLs). If the power-division ratios are not 0 dB for the same termination impedances, the two TLs should be identical, and the other two should have the same characteristic impedances for an electrical length difference of 180°. If, for example, the power-division ratio is 12 dB with the termination impedance of 50 Ω, the characteristic impedances of TLs should be 205.24 and 51.56 Ω [9, eq. (1)], and all TLs should be as short as possible due to compactness requirements. However, the TLs with the characteristic impedance of 205.24 Ω do not seem to be easy to fabricate with a microstrip technology due to a required width of around or below 40 μm for commonly used substrates (e.g., for the prototype discussed in this brief, the required microstrip linewidth was 42 μm for a substrate with a thickness of 20 mil and a dielectric constant 2.2), whereas the physical length of the low-impedance (51.26 Ω) TLs should be reduced without a significant bandwidth compromise. Due to the aforementioned implementation difficulties, most of previously reported efforts have treated the compact ring hybrids for equal power divisions [1], [3], [4] or for power-division ratios less than or equal to 6 dB [5]. In [6], high power-division ratios have been treated, but the size is not compact, and the demanded power-division ratio is achieved only around the design frequency. In [7], a prototype for the power-division ratio of 9.54 dB has been presented; nevertheless, it requires as many as four chip inductors and features a smaller bandwidth than the proposed topology. In [8], the 12-dB power-division ratio has been treated, and equivalent/artificial lumped-element TL models have been suggested for high-impedance TLs. However, the extraction method for the lumped-element values seems to be very complicated, and the bandwidth is much smaller than that of the conventional one, whereas the size is not compact. The power-division ratio of 13 dB has been investigated [9], but the size (320.58°) is not compact, as well.

In this brief, a novel compact wideband ring hybrid allowing the realization of arbitrarily high power-division ratios in a miniaturized form factor will be introduced. In the preliminary ring design, for a proof-of-concept 12-dB power-division ratio prototype, we assume that it includes two high-impedance TLs, which effectively are 90° and 270° long, and two low-impedance 90° TLs, and each TL should be as miniaturized as possible. However, the size reduction approach should be different for every TL, and conventional ways, such as T- and Π-types [12, Fig. 6 with $N = 1$], cannot be applied for this case, due to their inherent lack of a mechanism to reduce high-impedance values to easier-to-realize lower ones.

To overcome these issues, the high-impedance TL of the effective length of 270° can be reduced to a set of coupled TLs, which is physically less than 90° long but can also feature an additional inherent wideband 180° phase shift, whereas the high-impedance 90° TL is shortened by the use of an L_{s1}-section type configuration [9] that allows the simultaneous reduction of the characteristic impedance value. The two low-impedance TLs are miniaturized through the use of modified T-section types (MT-section types). Using the respective equivalent circuits of these three utilized topologies, a coupled-line ring hybrid prototype was easily fabricated at the design frequency of 1 GHz, and the total electrical length of the fabricated prototype was 209.3°, which occupies only 15% of the area

Manuscript received June 13, 2016; revised July 18, 2016; accepted July 24, 2016. Date of publication August 4, 2016; date of current version May 26, 2017. This brief was recommended by Associate Editor Z. Galias.

The authors are with the School of Electrical and Computer Engineering, Georgia Institute of Technology, Atlanta, GA 30332-250 USA (e-mail: hranahn@gmail.com; etentze@ece.gatech.edu).

Color versions of one or more of the figures in this brief are available online at http://ieeexplore.ieee.org.

Digital Object Identifier 10.1109/TCSII.2016.2598227

1549-7747 © 2016 IEEE. Personal use is permitted, but republication/redistribution requires IEEE permission.
See http://www.ieee.org/publications_standards/publications/rights/index.html for more information.

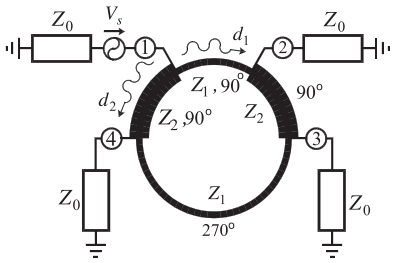

Fig. 1. Ring hybrid topology for arbitrary power-division ratios ($d_1 \neq d_2$).

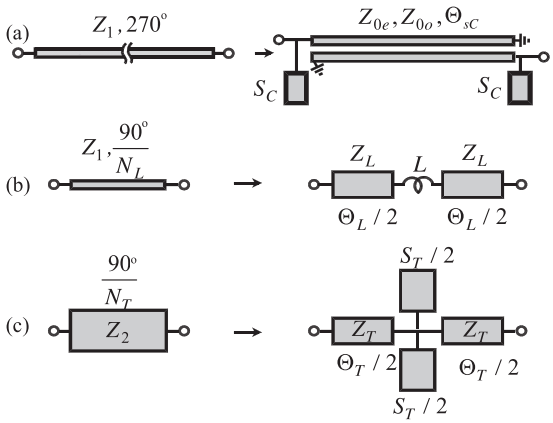

Fig. 2. Miniaturization equivalent circuits. (a) $C\Pi$-section type for a 270° high-impedance (Z_1) TL. (b) L_{s1}-unit block for a ($90°/N_L$) high-impedance (Z_1) TL. (c) MT-unit block for a ($90°/N_T$) low-impedance (Z_2) TL.

occupied by the conventional design. The measured bandwidth with a 15-dB return loss is 78%, a significantly higher value, as compared with the conventional one of 44%.

II. Miniaturization Approach/Equivalent Circuits

The topology of a typical ring hybrid with the same termination impedance Z_0 for all its ports is depicted for an arbitrary power-division ratios in Fig. 1; it consists of three 90° and one 270° TLs with the characteristic impedances of Z_1 and Z_2. For the proof-of-concept power-division ratio (d_2^2/d_1^2) of 12 dB with $Z_0 = 50\,\Omega$, the characteristic impedances of Z_1 and Z_2 are 205.24 and 51.56 Ω, respectively, [9], and the length of every TL should be reduced for compactness. Fig. 2 presents various compact topologies that effectively realize the 90° and 270° electrical lengths, although their physical length corresponds to much shorter electrical lengths. The 270° TL with the high impedance of Z_1 in Fig. 2(a) can be miniaturized using a set of coupled TLs with the even- and odd-mode impedances of Z_{0e} and Z_{0o} and the electrical length of Θ_{sC} and two shunt open stubs. The electrical length of Θ_{sC} is much shorter than 90°, and the susceptance of each open stub is denoted by S_C.

The equivalent circuit in Fig. 2(a) is named coupled-line Π-section type ($C\Pi$-section type). The high-impedance (Z_1) TL with an electrical length of $90°/N_L$ (N_L: arbitrary integer) in Fig. 2(b) can be miniaturized with the L_{s1}-unit block being composed of two identical TLs with Z_L and $\Theta_L/2$ interconnected with one series inductance L. The low-impedance (Z_2) TL with an electrical length of $90°/N_T$ (N_T: arbitrary integer) in Fig. 2(c) can be shortened with the MT-unit block comprising of two identical TLs with the characteristic impedance of Z_T and the electrical length of $\Theta_T/2$ and two identical shunt stubs of individual susceptance of $S_T/2$ in between. The integers N_L and N_T of the L_{s1}- and MT-section unit cells are typically smaller than 5 and represent the numbers of unit cells required to effectively realize the aggregate electrical lengths of 90° for the high- and low-impedance TLs, respectively.

The design formulas for the parameters of the $C\Pi$-section type and of the unit blocks of the L_{s1}- and MT-section types [9], [12] are

$$Z_{0e} = Z_1 \frac{1}{\sin\Theta_{sC}} \frac{C}{1-C}, \quad Z_{0o} = Z_1 \frac{1}{\sin\Theta_{sC}} \frac{C}{1+C} \tag{1a}$$

$$S_C = \frac{\cos\Theta_{sC}}{C \cdot Z_1} \tag{1b}$$

$$Z_L = Z_1 \frac{\tan\frac{\Theta_L}{2}}{\tan\frac{\pi}{4N_L}}, \quad \omega_0 L = 2Z_1 \frac{\tan^2\frac{\pi}{4N_L} - \tan^2\frac{\Theta_L}{2}}{\tan\frac{\pi}{4N_L} + \tan^3\frac{\pi}{4N_L}} \tag{1c}$$

$$Z_T = Z_2 \frac{\tan\frac{\pi}{4N_T}}{\tan\frac{\Theta_T}{2}} \tag{1d}$$

$$S_T = \frac{2}{Z_T} \cdot \frac{Z_T - Z_2 \cot\frac{\pi}{4N_T}\tan\frac{\Theta_T}{2}}{Z_T \tan\frac{\Theta_T}{2} + Z_2 \cot\frac{\pi}{4N_T}} \tag{1e}$$

where C is the target coupling coefficient, and ω_0 is the design angular frequency.

III. Validating Ring Hybrid Designs for Power-Division Ratio of 12 dB

Equations (1a) and (1b) imply that the values of Z_{0e}, Z_{0o}, and S_C are determined by the electrical lengths of Θ_{sC} for a fixed value of C. For the design of an L_{s1}-unit block in Fig. 2(b), the characteristic impedance of Z_L should be sufficiently lower than Z_1, so that it can be realized without any difficulty, and the inductance values of L should be easily fabricated with available off-the-shelf inductors (e.g., 0402 chip inductors) that typically require microstrip linewidths of the (Z_L) TLs on the order of 500 μm. The characteristic impedances of Z_T of the MT-unit blocks in Fig. 2(c) are inversely proportional to the electrical lengths of Θ_T. For the substrate (RT/Duroid 5880, $\varepsilon_r = 2.2$, $H = 20$ mil) used in the proof-of-concept prototype, the required linewidth is around 450 μm for the characteristic impedance value of 100 Ω. Therefore, the highest characteristic impedance values of Z_L and Z_T are set to around 100 Ω to enable the easy soldering of the chip inductors in between the two TLs.

Numerous values of the characteristic impedances of Z_L and Z_T are calculated in Tables I and II by varying the aggregate electrical length $N_i\Theta_i$ of the L_{s1}- and MT-section types, which is kept constant for different number of utilized stages N_i, where i is L or T, used for the implementation of the high-/low-impedance TLs with a total effective phase delay of 90°.

Table I shows that for the proof-of-concept prototype, characteristic impedance Z_L values around 100 Ω can be obtained for the design value $N_L\Theta_L = 45°$. In this case, for $N_L = 2, 3,$ and 4, the inductance values of L are, based on (1c), calculated as 17.77, 12.39, and 9.43 nH at 1 GHz, leading to the total

TABLE I
CALCULATED VALUES OF Z_L OF L_{s1}-SECTION TYPES

	$N_L\Theta_L = 45^\circ$	$N_L\Theta_L = 50^\circ$	$N_L\Theta_L = 60^\circ$
	Z_L (Ω)	Z_L (Ω)	Z_L (Ω)
$N_L = 2$	98.56	109.85	132.77
$N_L = 3$	100.94	112.20	135.06
$N_L = 4$	101.63	113.00	135.84

TABLE II
CALCULATED VALUES OF Z_T OF MT-SECTION TYPES

	$N_T\Theta_T = 40^\circ$	$N_T\Theta_T = 50^\circ$	$N_T\Theta_T = 60^\circ$
	Z_T (Ω)	Z_T (Ω)	Z_T (Ω)
$N_L = 2$	105.12	96.32	79.69
$N_L = 3$	118.18	94.31	78.34
$N_L = 4$	117.21	96.63	77.89

TABLE III
DESIGN DATA OF $C\Pi$-SECTION TYPES

$C\Pi$-section type for 270° TL with $Z_1 = 205.24$ Ω, $C =$ -10 dB			
Θ_{sC}	Z_{0e}	Z_{0o}	${S_C}^{-1}$
85°	95.27 Ω	49.49 Ω	744.66 Ω
75°	98.26 Ω	51.05 Ω	250.76 Ω
65°	104.73 Ω	54.41 Ω	153. 57 Ω

inductance values of $N_L * L$ being 35.54, 37.17, and 37.74 nH, respectively. The values of $N_L * L$ should be as small as possible, and therefore $N_L = 2$ is desirable. However, $L = 17.77$ nH is impossible to realize with off-the-shelf components, the closest of which is 18 nH. Fixing $N_L = 2$ and $L = 18$ nH, the electrical length of $N_L\Theta_L$ can be easily calculated as $N_L\Theta_L = 44.27^\circ$ from (1c). From the data in Table II, it can be easily observed that the values of the characteristic impedance Z_T around 100 Ω can be obtained for design lengths $N_T\Theta_T$ between 40° and 50°.

Following the approach discussed in [2, Figs. 2 and 3], it can be easily shown that for the proof-of-concept prototype presented in this brief, the 90° and 270° high-impedance (Z_1) TLs are impedance transformers that each convert an impedance of 842.45 Ω into the termination impedance of 50 Ω, and the two low-impedance (Z_2) TLs are transforming 53.16 into 50 Ω. Based on the presented design concept, i.e., (1a)–(1e) and the data in Tables I and II, the design parameters for the $C\Pi$-, L_{s1}-, and MT-section types are listed in Tables III–V, respectively. For the utilized $C\Pi$-section types, the coupling coefficient is fixed at −10 dB, and the electrical lengths of Θ_{sC} are varied, because the gap width is greater than 100 μm for such a coupling coefficient on the same substrate and therefore can be fabricated without any difficulty. For the utilized L_{s1}-section types, the total length of $N_L\Theta_L$ is fixed at 44.27°, and the number of N_L is varied. For the utilized MT-section types, the total length of $N_T\Theta_T$ is fixed at 45°, and the number of N_T is varied.

The frequency responses were simulated at the design frequency of 1 GHz for the design data in Tables III–V and are plotted in Fig. 3, where the $C\Pi$- and L_{s1}-section types are terminated in 842.45 and 50 Ω, whereas the MT-section types are terminated in 53.155 and 50 Ω, and the susceptances of S_C and S_T were realized with capacitances at 1 GHz. The

TABLE IV
DESIGN DATA OF L_{s1}-SECTION TYPES

L_{s1} − section type for 90° TL with $Z_1, N_L\Theta_L = 44.27^\circ$			
N_L	Z_L	Θ_L	$\omega_0 L$
1	83.48 Ω	44.27°	171.28 Ω
2	96.92 Ω	22.13°	112.76 Ω
3	99.18 Ω	14.76°	78.65 Ω

TABLE V
DESIGN DATA OF MT-SECTION TYPES

MT − section type for 90° TL with $Z_2, N_T\Theta_T = 45^\circ$			
N_T	Z_T	Θ_T	${S_T}^{-1}$
2	107.35 Ω	22.5°	94.76 Ω
3	104.93 Ω	15.0°	135.92 Ω
4	104.12 Ω	11.25°	178.47 Ω

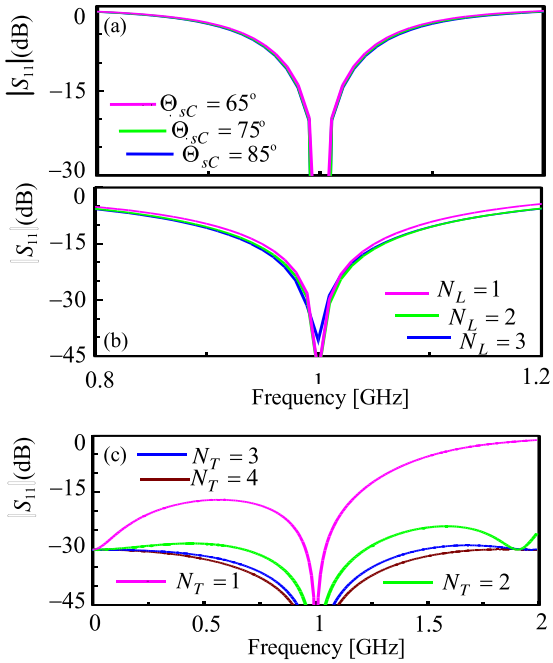

Fig. 3. Frequency responses. (a) $C\Pi$-section types. (b) L_{s1}-section types. (c) MT-section types.

frequency responses of the $C\Pi$-section types in Fig. 3(a) feature a similar behavior, regardless of the electrical lengths of Θ_{sC} between 65°–85°; that allow the even-mode characteristic impedance values of around or below 100 Ω in very miniaturized implementations. The frequency responses of the L_{s1}-section types with $N_L = 2$ and 3 in Fig. 3(b) are about the same, whereas that of the L_{s1}-section type with $N_L = 1$ is slightly worse than the other two. For the MT-section types in Fig. 3(c), the performance for the one with $N_T = 4$ is the best.

In terms of compactness, minimum radiation loss, easy fabrication and broadband operability, the number of required unit blocks N_L and N_T, as well as the required phase Θ_{sC} were optimized for the fabrication of the prototype. The $C\Pi$-section type with $\Theta_{sC} = 75^\circ$ was chosen, because despite the fact it is not the shortest, the value of its respective ${S_C}^{-1}$ can be easily fabricated with a TL and an available chip capacitor. The L_{s1}-section type with $N_L = 2$ was selected because the

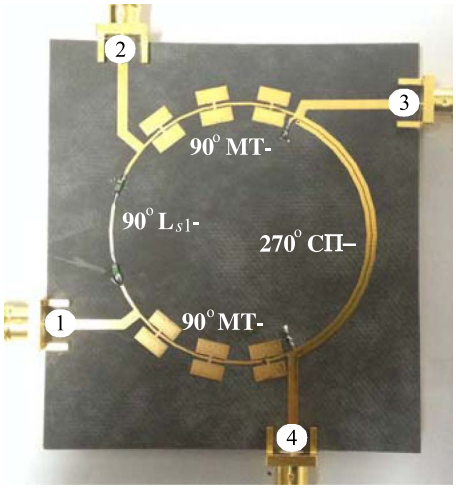

Fig. 4. Fabricated compact coupled-line ring hybrid prototype.

required inductance at 1 GHz can be easily realizable with available off-the-shelf chip inductors of 18 nH as previously mentioned. The MT-section type with $N_T = 4$ features in Fig. 3(c) a slightly better performance than that with $N_T = 3$ but both have a return loss better than 30 dB in the whole frequency range of interest. However, the individual unit block's electrical length of Θ_T with $N_T = 4$ is shorter than that with $N_T = 3$, which causes a significant difficulty to realize ${S_T}^{-1}$ only with distributed elements. Due to the reason, the MT-section type with $N_T = 3$ was chosen.

IV. Fabrication, Measurements, and Comparison

Based on the selected and optimized section types from the data in Tables III–V, a compact ring hybrid was fabricated on a commonly used substrate, and the resulting prototype is demonstrated in Fig. 4, where the 90° MT- and L_{s1}-section types are 45° and 44.27° long, the 270° $C\Pi$-section type is 75° long, each susceptance of S_C was realized with a TL and a chip capacitor with 0.5 pF similar to the form in [4, Fig. 13(a)], whereas the chip inductors with the inductance value of 18 nH (0402 Murata, LQW15AN18NJ80, Rdc; 0.13 Ω, tolerance; ±5%, SRF(min); 5.2 GHz) were soldered, and each $S_T/2$ was fabricated with an open-circuited high–low stepped impedance TL. The measured responses are compared with the predicted ones in Fig. 5. The measured bandwidth with a 15-dB return loss at port ① is 78% (0.65–1.43 GHz) in Fig. 5(a), that with 15-dB isolation in Fig. 5(b) is 147% (0–1.47 GHz), that with the power-division ratio of 11.5–12.5 dB is 78% (0.75–1.19 GHz, 1.25–1.59 GHz) in Fig. 5(c), whereas the phase responses in Fig. 5(d) also show wideband performance. Given the fabrication errors, the measured results are in good agreement with the predicted ones, indicating that the usage of the chip inductors and capacitors is acceptable for this application even for typical tolerances and parasitic elements.

The measured frequency responses of the fabricated prototype are compared in Fig. 6 with the simulated ones of a much larger conventional one for the same power-division ratio of 12 dB that was simulated with ideal parameter values. The input matching, isolation, power-division ratios and phase difference

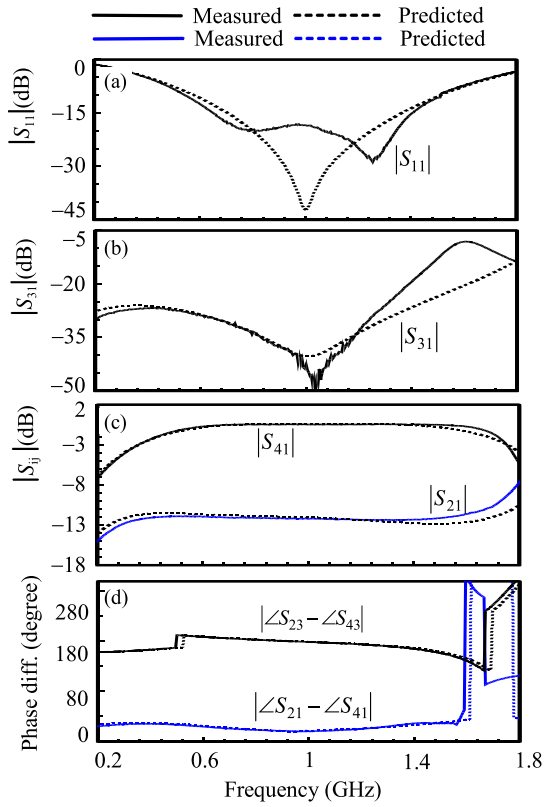

Fig. 5. Compared measured and predicted frequency responses. (a) $|S_{11}|$. (b) $|S_{31}|$. (c) Power divisions. (d) Phase responses.

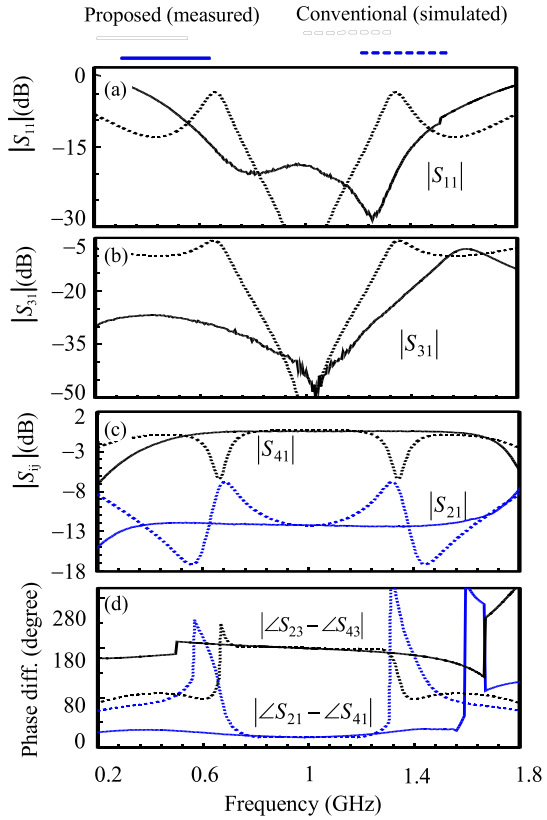

Fig. 6. Comparison of the proposed compact ring hybrid with the conventional one. (a) Input matching of $|S_{11}|$. (b) Isolation of $|S_{31}|$. (c) Power division to ports 2 and 4. (d) In-phase and out-of-phase differences.

TABLE VI
COMPARED FREQUENCY RESPONSES

Frequency performance	Proposed (measured)	Conventional (simulated)
15-dB return loss BW	78 %	44 %
15-dB isolation BW	147 %	52 %
power division ratios (12± 0.5) dB	78 %	21 %
out-of-phase difference $180^{o} \pm 10^{o}$	76 %	60 %
in-phase difference $0^{o} + 10^{o}$	70.4 %	52%

frequency responses are shown in Fig. 6(a)–(d), respectively. The compared responses are summarized in Table VI. The bandwidth with 15-dB return loss of the proposed one is 78%, whereas that of the conventional one is 44%. The bandwidth with the 15-dB isolation of the proposed one is 147%, whereas that of the conventional one is 52%. The bandwidths with the power-division ratios of (12 $\pm$ 0.5) dB of the proposed and conventional ones are 56% and 21%, respectively.

The bandwidths of the absolute out-of-(180°) and in-phase (0°) differences of the proposed one are 76% and 70.4%, whereas those of the conventional one are 60% and 52%. In terms of size, the conventional one consists of TLs with an aggregate length of 540°, whereas the circumference of the proposed one is only 209.27° long, leading to a drastic miniaturization to only 15% of the conventional area, while featuring a much more wideband performance.

V. CONCLUSION

In this brief, a novel, compact, and wideband ring hybrid was introduced for the easy realization of arbitrarily high power-division ratios. The proposed topology miniaturizes the size by utilizing $C\Pi$-, L_{s1}- and MT-section topologies. The circumference of one fabricated proof-of-concept 12-dB power-division ratio prototype is only 209.3° long, as compared with 540° of conventional implementations verifying an area miniaturization down to 15%, whereas the measured bandwidth of the 15-dB return loss is 78% versus the conventional one's 44%, an improvement by a factor 1.8. The topology introduced in this brief could be easily optimized for a wide range of power-division ratios and could set the foundation for the implementation of similar ultra miniaturized hybrids to a variety of wearable, implantable, Internet of Things, and aerospace applications.

REFERENCES

[1] H.-R. Ahn, I.-S. Chang, and S. Yun, "Miniaturized 3-dB ring hybrid terminated by arbitrary impedances," *IEEE Trans. Microw. Theory Tech.*, vol. 42, pp. 2216–2221, Dec. 1994.
[2] H.-R. Ahn, I. Wolff, and I.-S. Chang, "Arbitrary termination impedances, arbitrary power division, and small-sized ring hybrids," *IEEE Trans. Microw. Theory Tech.*, vol. 45, pp. 2241–2247, Dec. 1997.
[3] H.-R. Ahn and B. Kim, "Small wideband coupled-line ring hybrids with no restriction on coupling power," *IEEE Trans. Microw. Theory Tech.*, vol. 57, no. 7, pp. 1806–1817, Jul. 2009.
[4] H.-R. Ahn and S. Nam, "Compact microstrip 3-dB coupled-line ring and branch-line hybrids with new symmetric equivalent circuits," *IEEE Trans. Microw. Theory Tech.*, vol. 61, no. 3, pp. 1067–1078, Mar. 2013.
[5] C.-L. Hsu, J.-T. Kuo, and C.-W. Chang, "Miniaturized dual-band hybrid couplers with arbitrary power division ratios," *IEEE Trans. Microw. Theory Tech.*, vol. 57, no. 1, pp. 149–156, Jan. 2009.
[6] M.-J. Park and B. Lee, "Design of ring couplers for arbitrary power division with 50 Ω lines," *IEEE Microw. Wireless Compon. Lett.*, vol. 21, no. 4, pp. 185–187, Apr. 2011.
[7] M. M. Honari, R. Mirzavand, P. Mousavi, and A. Abdipour, "Class of miniaturised /arbitrary power division ratio couplers with improved design flexibility," *IET Microw. Antennas Propag.*, vol. 9, pp. 1066–1073, 2015.
[8] K.-L. Ho and P.-L. Chi, "Miniaturized and large-division-ratio ring coupler using novel transmission-line elements," *IEEE Microw. Wireless Compon. Lett.*, vol. 24, no. 1, pp. 35–37, Jan. 2014.
[9] H.-R. Ahn and S. Nam, "Wideband microstrip coupled-line ring hybrids for high power-division ratios," *IEEE Trans. Microw. Theory Tech.*, vol. 61, no. 5, pp. 1768–1780, May 2013.
[10] Y. Wang, M. Koen, and D. Ma, "Low-noise CMOS TGC amplifier with adaptive gain control for ultrasound imaging receivers," *IEEE Trans. Circuit Syst. II. Exp. Briefs*, vol. 58, no. 1, pp. 26–30, Jan. 2011.
[11] C. Zhou, L. Zhang, L. Zhang, Y. Wang, Z. Yu, and H. Qian, "Injection-locking-based power and speed optimization of CML dividers," *IEEE Trans. Circuit Syst. II. Exp. Briefs*, vol. 58, no. 9, pp. 565–569, Sep. 2011.
[12] H.-R. Ahn and S. Nam, "New design formulas for impedance-transforming 3-dB Marchand baluns," *IEEE Trans. Microw. Theory Tech.*, vol. 59, pp. 2816–2823, Nov. 2011.